SOIL SCIENCE ANNUAL
2025, 76(2), 207727

https://doi.org/10.37501/soilsa/207727

The drying of the Aral Sea: Soil formation and restoration potential on the seabed

Zafarjon Jabbarov[1], Shovkat Kholdorov*[1], Zafarjon Jabbarov[1], Urol Nomozov[2], Samad Makhammadiev[1], Gulnora Djalilova[1], Shokhrukh Abdullaev[1]

[1] National University of Uzbekistan named after Mirzo Ulugbek, Faculty of Biology, Department of Soil Science, Almazar district, University Street, 4th house, 100174, Tashkent, Uzbekistan

[2] Tashkent branch of the Samarkand state university veterinary medicine of livestock and biotechnologies, Chilanzar district 20, house 35a3, Tashkent, Uzbekistan

* Corresponding author: Shovkat Kholdorov, sh.m.xoldorov@gmail.com, ORCID iD: https://orcid.org/0000-0001-9394-215X

Received: 2024-12-14
Accepted: 2025-06-30
Published online: 2025-06-30
Associated editor: Cezary Kabała

Keywords:

Aral Sea drying
Seabed soil salinity
Adaptive vegetation strategies
Site-specific management
Soil composition

Abstract

The drying of the Aral Sea has exposed vast seabed areas characterized by heterogeneous soils influenced by climatic, hydrological, and ecological factors. This research analyzed the physical, chemical, and nutrient properties of soils from ten profiles that illustrate different stages of the Aral Sea's retreat. The results revealed substantial spatial variation in soil properties, including particle-size distribution, salinity, organic matter, and nutrient content. While earlier exposure profiles generally exhibited finer textures, lower salinity (EC), and higher organic matter content, nutrient distribution (N, P, K) did not follow a consistent age-related trend. Instead, elevated nutrient levels were observed in profiles across all exposure stages, highlighting the influence of vegetation input and localized site conditions. Salinity has been identified as a significant factor impeding soil development and vegetation establishment, exhibiting strong negative correlations with organic matter and nutrient retention. Surface salinity and nutrient depletion were most severe in the top 0–5 cm layer; mulching may help improve conditions for plant establishment. These findings emphasize the need for site-specific restoration planning based on measured soil characteristics. Areas with suitable soil conditions may grow drought-resistant species, whereas regions characterized by high salinity or degradation necessitate halophytes that are adapted to low fertility and extreme environmental conditions. These insights provide critical guidance for the implementation of targeted, site-specific restoration projects focused on soil stabilization, biodiversity enhancement, and desertification mitigation in the Aral Sea region.

1. Introduction

Salt-affected soils cover 1,381 million hectares, representing 10.7% of the global land area, with an additional 1,038 million hectares at risk of salinization (EC 0.75–2 dS·m^{-1}). This situation presents a significant challenge to agriculture, ecosystems, and livelihoods. (FAO, 2024). Arid regions such as Central Asia exhibit heightened vulnerability, as soil salinity exacerbates the process of desertification. In Uzbekistan, approximately 50% of irrigated arable land is currently affected by salinization, attributable to both natural and human-induced factors. (Kholdorov et al., 2023). The drying of the Aral Sea is a striking example of this crisis.

The Aral Sea, which once covered 68,000 km^2 between Uzbekistan and Kazakhstan, supported regional ecology and economies until its rapid decline starting in the 1960s (Kuziyev et al., 2020). While historical climate fluctuations—recorded as early as Herodotus (5th century BCE) and Al-Balkhi (9th century CE) – once influenced the sea's levels (UNESCO, 2017), modern desiccation has been overwhelmingly human-driven. Soviet-era irrigation policies diverted over 90% of the Amu Darya and Syr Darya rivers for cotton monoculture, using inefficient, unlined channels (Issanova et al., 2022; Massakbayeva et al., 2020). By 1989, the sea had split, and by 2020, it had shrunk to a tenth of its original size, exposing vast salt flats that generate 1,143–2,684 t/km^2 of airborne dust annually (Issanova et al., 2022).

The drying unfolded in distinct phases (Table 1, Fig. 1), starting in the southeast and east (1960s) and expanding westward and southward (1990s). This process accelerated salinization and desertification, fundamentally altering soil properties. In response, efforts to combat desertification include afforesting approximately 100,000 hectares of the exposed seabed with saxaul (*Haloxylon ammodendron*) and other arid-adapted spe-

Table 1
Stages of Aral Sea retreat and affected areas (1960–2014)

Period	Degree of Retreat	Affected Areas of the Aral Sea
1960	Beginning (Weak)	Southeast, East
1970	Strength Level	Southeast, East, Central-West, North
1980	Average Level	Southeast, South, East, Central-West, North
1990	Strength Level	Southeast, South, East, Central-West, North, Southwest
2000	Very Strong	Southeast, South, East, Central-West, North, Southwest
2004	Very Strong	Southeast, South, East, Central-West, North, Southwest
2008	Very Strong	Southeast, South, East, Central-West, North, Southwest, Central
2014	Very Strong	Southeast, South, East, Central-West, North, Southwest, Central

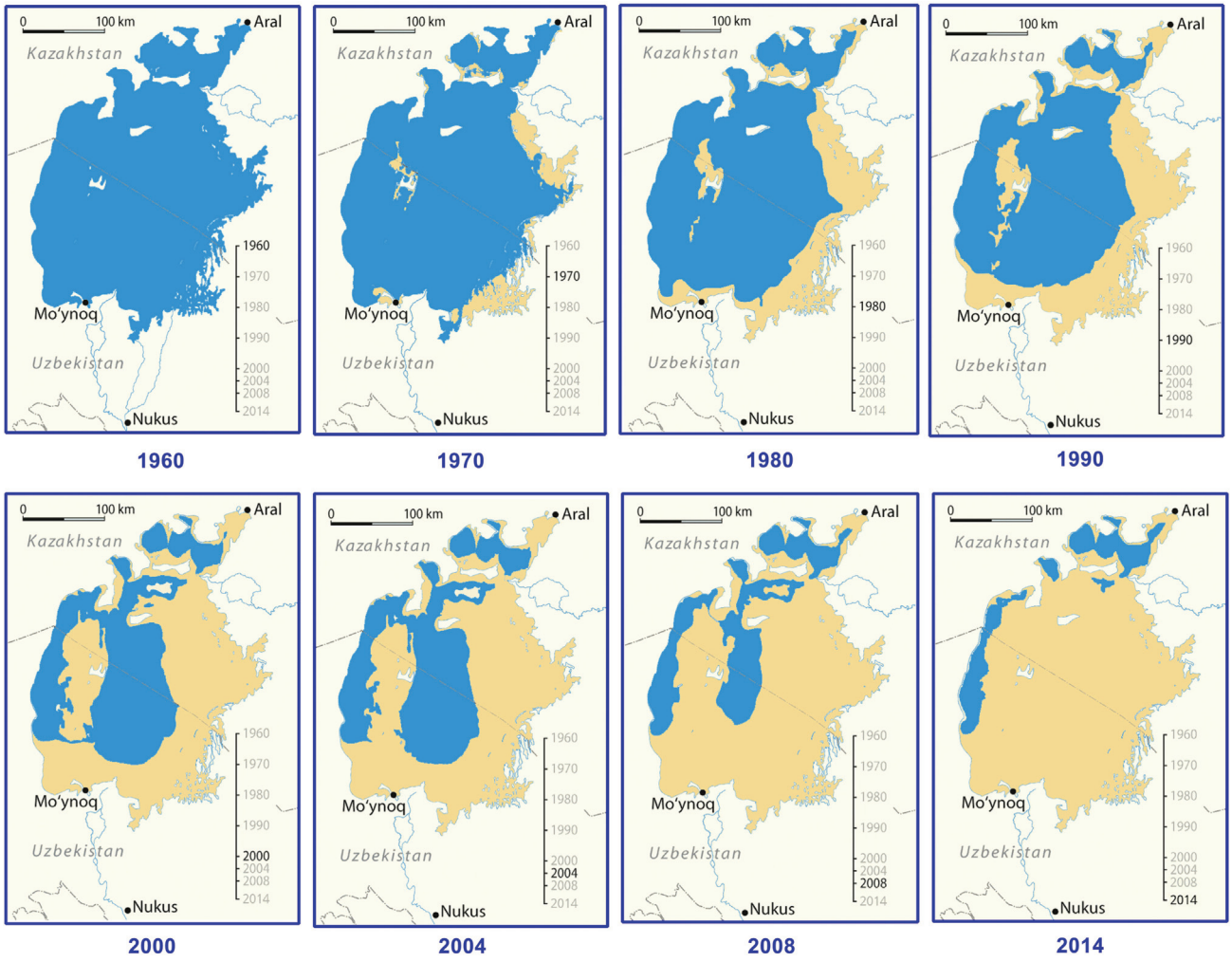

Fig. 1. The stages of Aral Sea retreat from 1960 to 2014 (Brilliant Maps, 2023)

cies annually. However, harsh soil conditions, marked by high salinity and low fertility, have limited vegetation establishment, highlighting the need for soil-specific restoration approaches.

Although extensive research has focused on hydrological and ecological impacts, there is a lack of systematic analysis regarding the soil characteristics of the seabed. This research aimed to analyze the soil characteristics of the Aral Sea's exposed seabed sediments, formed during various drying stages, to evaluate their suitability for vegetation-based restoration strategies. This study analyzed essential soil properties, such as particle size distribution, organic matter content, salinity, and nutrient levels (NPK), to identify areas with optimal conditions

for vegetation establishment and ecological restoration, rather than concentrating on soil formation processes.

2. Materials and methods

2.1. Study area and site selection

The study was conducted on the exposed southeastern seabed of the Aral Sea, located in Uzbekistan site. This area was chosen due to its early exposure in the 1960s, providing an opportunity to investigate soil formation under arid conditions. As the water receded, particularly from the southeastern and eastern regions, soil development began, with characteristics varying based on the duration of exposure. The study targeted ten soil profiles, each georeferenced with precise latitude and longitude coordinates, to capture the chronological phases of the sea's retreat, as shown in the drying evolution maps (Fig. 1). The sampling sites (Fig. 2) were strategically selected and arranged in a chronological sequence, reflecting the Aral Sea's drying history. Point 1 represents the earliest dried area, while Point 10 marks the most recently dried zone. These sites are distributed in a roughly linear pattern across the southeastern exposed seabed. This arrangement mirrors the historical retreat

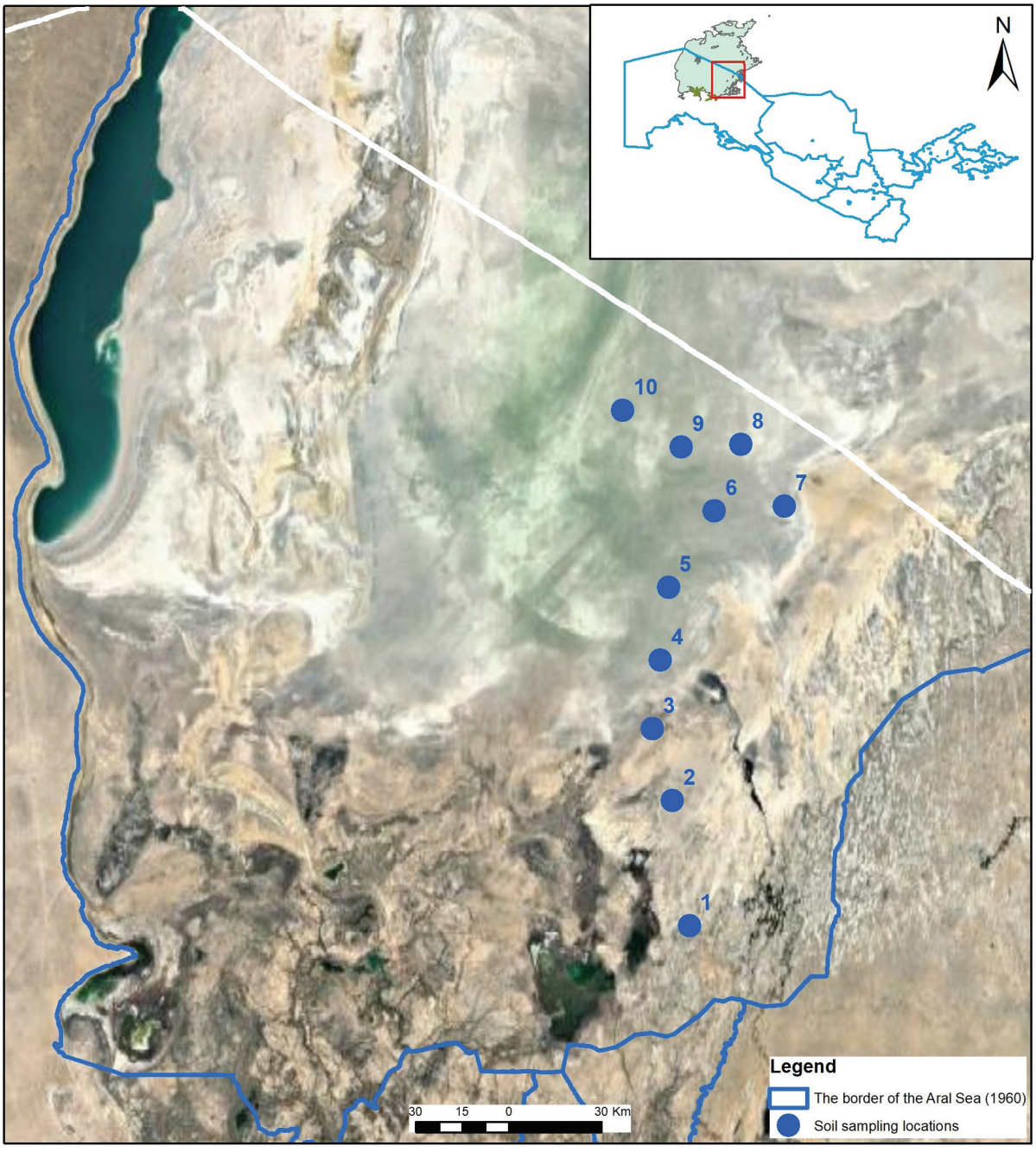

Fig. 2. Study area within the southeastern part of the dried Aral Sea

of the sea, allowing for a systematic analysis of soil evolution over time.

2.2. Soils and soil sampling

The soils in this region exhibit significant differences from typical zonal soil formation processes, mainly because of the harsh environmental conditions present in the Aral Sea area. To a significant degree, salt accumulation leads to the development of coastal salt flats, known as solonchaks, distinguished by their chloride, sulfate-chloride, and chloride-sulfate salinization patterns. Over time, these soils experience differentiation shaped by the lithological and morphological characteristics of the seabed. Fine sediments create aeolian landscapes that are susceptible to wind erosion. In contrast, denser substrates evolve into desert solonchaks, which may ultimately change into takyric soils or highly saline automorphic soils in arid regions.

We collected a total of 68 soil samples from 10 profiles (Fig. 2) in the south-eastern part of the dried seabed of the Aral Sea. These sampling locations were arranged sequentially to represent the chronological shrinkage of the sea. Each point was georeferenced to ensure spatial accuracy. At each location, soil samples were collected from multiple depth layers within the profiles. Most profiles extended to a depth of 120 cm. Samples were collected at the following depth layers: 0–5 cm, 5–15 cm, 15–30 cm, 30–50 cm, 50–70 cm, 70–90 cm, and 90–120 cm. This sampling method ensured consistent and detailed coverage of soil characteristics across different depths and site conditions. Sampling continued until a wet layer was encountered, marking the practical excavation limit due to the infeasibility of deeper digging. However, at Profile 3, sandy soil conditions restricted excavation depth, allowing for the collection of only four samples. The sampled depth layers ranged from the surface to subsurface, with precise top and bottom depths recorded in centimeters. This method ensured a comprehensive assessment of both horizontal and vertical variations in key soil properties, such as salinity, texture, and structure. The resulting dataset provides valuable insights into changes in soil characteristics over time as the Aral Sea receded.

After collection, soil samples were air-dried at room temperature (approximately 25°C) to remove moisture. The dried samples were then milled and sieved to achieve the required particle size for analysis.

2.3. Laboratory analysis

We analysed the soil samples using established procedures to determine their physical, chemical, and nutrient properties. Soil particle-size distribution was determined using the pipette method according to Kachinsky (Kachinsky, 1943). We determined the organic matter using the modified Tyurin method by CINAO, which involved oxidizing soil organic carbon with potassium dichromate, in accordance with GOST 26213-91 (Committee for Standardization and Metrology of the USSR, 1991). We determined the total phosphorus and potassium contents using acid digestion, following GOST 26261-84 (Ministry of Agriculture of the USSR, 1984a), and quantified them using spectrophotometry and flame photometry. We determined the total nitrogen content using the Kjeldahl method, as detailed in GOST 26107-84 (Ministry of Agriculture of the USSR, 1984b), which involved digestion with concentrated sulfuric acid and subsequent titration. Soil salinity was assessed by measuring electrical conductivity (EC) in a 1:1 soil-to-water suspension following the USDA method (United States Department of Agriculture, 1954)

3. Results

3.1. Soil particle-size distribution

Soil particle-size distribution results were grouped into sand (1.0–0.05 mm), silt (0.05–0.001 mm), and clay (<0.001 mm) fractions following the particle-size classification method by Kachinsky (1943), as shown in Fig. 3. Profiles 1 to 3, located in areas exposed during the early stages of the sea's desiccation, exhibited coarser surface textures and finer textures at depth. For example, in Profile 1, the surface layer (0–5 cm) contained 34.4% sand, 51.0% silt, and 14.6% clay, while the deeper layer (70–120 cm) showed an increased clay content, reaching 43.7%. Similarly, Profile 3, situated closer to the centre of the dried seabed, demonstrated the highest sand content among all profiles, with sand fractions reaching 49.3% in the 50–70 cm layer. This high sand content reflects high-energy hydrodynamic conditions that once dominated this region.

Profiles 4 to 7, representing the intermediate stages of shrinkage, displayed a transition from silt-dominated surface layers to sandier and more clay-rich layers at depth. For instance, sediment redeposition during fluctuating water levels led Profile 5 to exhibit the highest sand content (66.0%) in the 13–35 cm layer . Conversely, Profile 6 showed a gradual increase in clay content with depth, reaching 16.5% in the 90–120 cm layer. These profiles reflect the dynamic sedimentation conditions during periods of water level fluctuations in the Aral Sea's intermediate dried up phase. In profiles 8 through 10, which show the late shrinkage phase, the surface textures were dominated by silt, and the subsurface layers were more consistent in texture with depth. This suggests that the Aral Sea was settling down more slowly in its last stages. For instance, in Profile 8, 74.0% silt and 4.4% clay dominated the surface layer (0–5 cm), while deeper layers showed a slight increase in sand content (42.2% in the 30–50 cm layer). Profile 9 was characterized by high silt fractions, peaking at 68.9% in the 50–90 cm layer, with clay content increasing to 15.0% in the 90–120 cm layer.

3.2. Soil salinity

The measurement of electrical conductivity, as illustrated in Fig. 4, demonstrates the salinity distribution across all profiles, highlighting the variations in EC values by depth. Profile 1 demonstrated stable and moderate salinity values, with electrical conductivity consistently measured at 7.80 $dS \cdot m^{-1}$ across the depth range of 5 cm to 120 cm. Profiles 2 to 5 exhibited greater variability in salinity patterns. Profile 3 exhibited the highest surface EC value of 19.70 $dS \cdot m^{-1}$, which progressively decreased

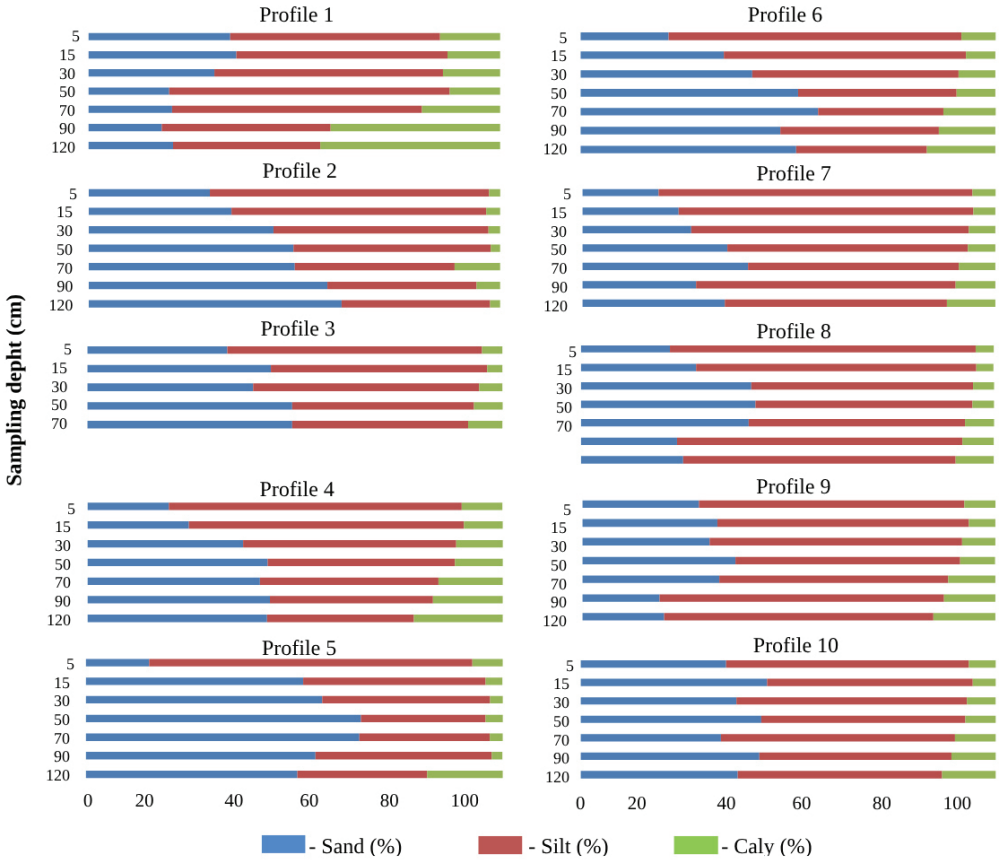

Fig. 3. Soil particle size distribution analysis across profiles from the dried up Aral Sea seabed

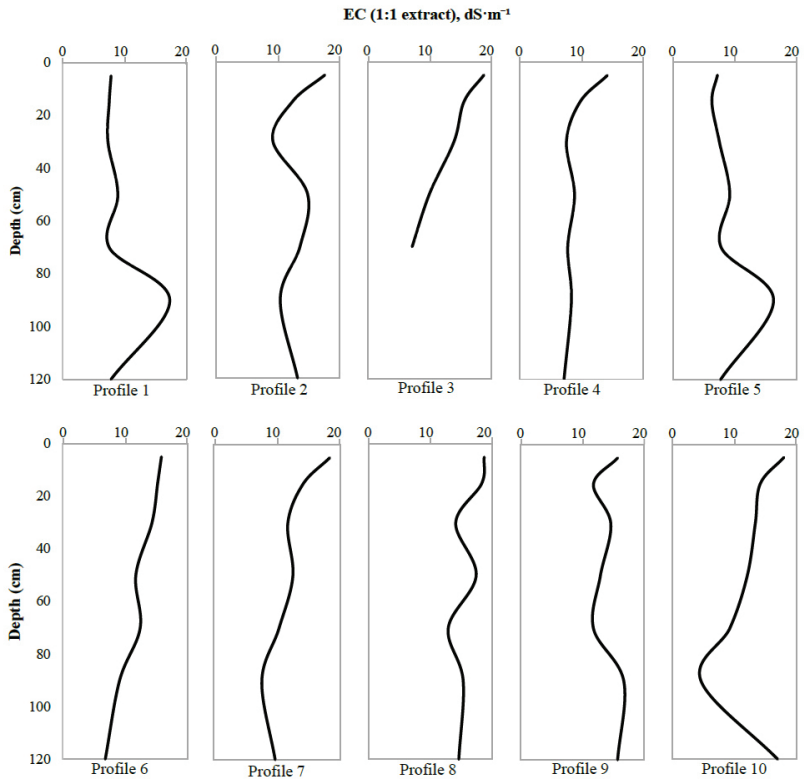

Fig. 4. Electrical conductivity (EC) analysis across profiles from the dried-up Aral Sea seabed

to 17.50 dS·m^{-1} at the 30–50 cm depth layer. Profile 2 exhibited consistently elevated EC values throughout various depths, with measurements ranging from 19.40 dS·m^{-1} at the 5 cm layer to 18.30 dS·m^{-1} at 120 cm. Profile 5 demonstrated a significant rise in EC from 7.20 dS·m^{-1} at the 0–5 cm depth to 16.30 dS·m^{-1} at the 70–90 cm layer, whereas Profile 4 maintained consistently moderate EC values. Profiles 6 and 7 exhibited moderate salinity levels characterized by notable deep fluctuations. Profile 6 exhibited a gradual decline in EC from 15.80 dS·m^{-1} at the 0–5 cm layer to 6.80 dS·m^{-1} at the 90–120 cm layer. Profile 7 exhibited an initial electrical conductivity of 18.30 dS·m^{-1} at the surface, which decreased to 10.30 dS·m^{-1} within the 50–70 cm layer, followed by a subsequent increase to 9.70 dS·m^{-1} at the 90–120 cm layer. Profiles 8, 9, and 10 demonstrated the most pronounced and irregular salinity trends. Profile 8 exhibited an EC value of 18.70 dS·m^{-1} at the 0–5 cm layer, with negligible decreases observed at greater depths. Profile 9 exhibited irregular salinity patterns at increased depths, with a surface EC of 15.70 dS·m^{-1}. Profile 10 exhibited an EC value of 18.00 dS·m^{-1} at the surface, decreasing to 4.60 dS·m^{-1} at the 70–90 cm layer, and subsequently increasing to 17.00 dS·m^{-1} at the 90–120 cm layer.

3.3. Soil organic matter (SOM)

The amounts of SOM differed across profiles, resulting in three separate categories based on surface enrichment and depth dispersion (Fig. 5). Profiles 1, 5, and 9 had the greatest SOM concentrations, with surface values ranging from 0.33% to 0.38%, and a steady decrease with depth, indicating active biological contribution and organic buildup. Profiles 4, 6, 8, and 10 were categorized as moderate, with surface concentrations ranging from 0.25% to 0.30%, with a rather stable vertical trend. Profiles 2, 3, and 7 had the lowest SOM concentrations, often between 0.12% and 0.22%, with little change with layers. In Profiles 1, 4, 5, and 9, SOM concentrations were reduced in the topsoil (0–5 cm), increased in the subsurface layers (15–50 cm), and then decreased at increasing depths, resulting in a mid-depth peak. Conversely, Profiles 2, 3, 6, 7, 8, and 10 exhibited either the greatest surface amount of SOM or a more homogeneous vertical distribution, without significant enrichment within the upper layer.

3.4. Nutrient content (total nitrogen, phosphorus, and potassium)

Total nitrogen contents exhibited variability across profiles, often with a declining trend with increasing depth (Fig. 6). The profiles were categorized into four groups based on concentration levels. Profiles 1, 5, and 9 showed the greatest nitrogen concentrations, regularly attaining or surpassing 0.11% at various depths, with a peak of 0.13% in Profile 9 at 30–50 cm. Profiles 4 and 8 were designated as moderate, with values between 0.06% and 0.09% in the top layers, followed by a progressive decrease with depth. Profiles 3, 6, and 10 exhibited reduced nitrogen concentrations, typically ranging from 0.04% to 0.06%, with no vertical fluctuation. Profiles 2 and 7 had the lowest quantities, with nitrogen continuously low throughout deeper layers, ranging from 0.02% to 0.04%. Nitrogen concentrations in Profiles 1, 5, 6, and 9 decreased in the surface layer (0–5 cm) compared to the subsurface layers (15–50 cm), exhibiting different mid-depth

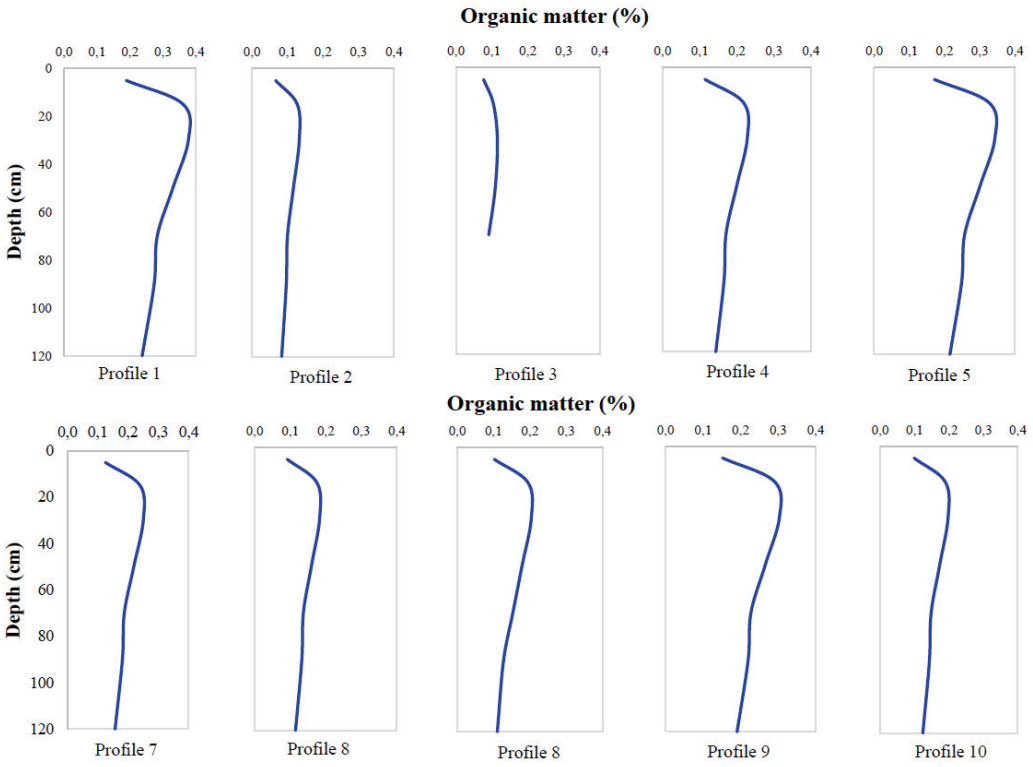

Fig. 5. Organic matter distribution analysis across profiles from the dried-up Aral Sea seabed

Fig. 6. Total Nitrogen (%) distribution across profiles from the dried-up Aral Sea seabed

peaks. Profiles 2 and 7 showed generally low nitrogen values across the profile, whereas Profiles 3, 4, 8, and 10 exhibited relatively stable distributions with minimal vertical variation.

Total phosphorus concentrations shown significant variability between profiles, generally decreasing with depth (Fig. 7). The profiles were classified into four categories based on concentration patterns. Profiles 1, 5, and 9 showed the greatest phosphorus concentrations, with maximum values of 0.38%, 0.34%, and 0.30%, respectively, and consistently high levels (≥0.27%) throughout several layers. Profiles 4, 6, and 10 were categorized

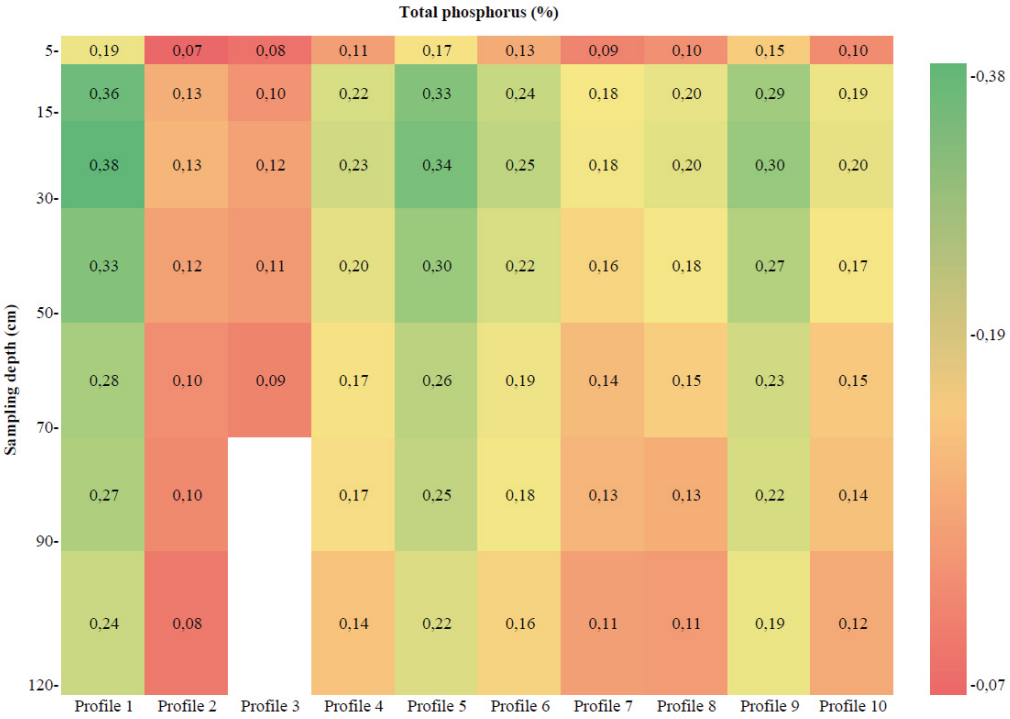

Fig. 7. Total phosphorus (%) distribution across profiles from the dried-up Aral Sea seabed

as moderate, with phosphorus concentrations typically between 0.17% and 0.25%, with little change over depth. Profiles 3, 7, and 8 constituted the low group, with concentrations mostly ranging from 0.11% to 0.16%, and devoid of any significant peak. Profile 2 was notably the lowest, sustaining phosphorus concentrations below 0.13% at all depths, with a minimum of 0.07% in the top layer. In nearly all profiles, phosphorus concentrations in the surface layer (0–5 cm) were lower than those in the subsurface layers, which ranged from 15 to 50 cm. The trend of subsurface enrichment was particularly noticeable in Profiles 1, 5, and 9; even in low-content profiles, the highest values were not found near the surface.

Total potassium values shown significant variability between profiles, allowing categorization into four separate groups (Fig. 8). Profiles 1, 5, and 9 were categorized as high-potassium profiles, exhibiting consistently high concentrations at all depths. Peak values above 2.00% in Profiles 1 and 5, although Profile 9 had a maximum of 1.84%, with all values remaining above 1.46%. Profiles 3, 4, 6, and 10 were classified as moderate, with consistent concentrations typically between 1.20% and 1.50%, with little fluctuation throughout layers. Profiles 7 and 8 constituted the low group, with potassium values mostly ranging from 0.98% to 1.11%, with no notable accumulation at depth. Profile 2 was designated as the lowest, demonstrating the minimal values in the dataset, regularly fluctuating between 0.64% and 0.81%. In 8 out of 10 profiles, potassium reaches its peak in deeper layers, particularly at 70–120 cm. Profile 3 shows a slight difference, with surface values being slightly higher than those at depth, whereas Profile 8 exhibits nearly uniform values with no significant vertical variation. The topsoil (0–5 cm) is not the highest in any profile.

4. Discussion

The drying of the Aral Sea exemplifies a complex environmental catastrophe influenced by the interplay of meteorological, human, geopolitical, and socioeconomic factors. This study's results, obtained from the analysis of soil profiles exhibiting different drying levels, reveal distinct variations in soil properties closely associated with the timing and conditions of exposure. The integration of these observations provides a comprehensive understanding of the factors affecting the formation of the parched bottom and highlights potential strategies for effective rehabilitation.

Climate variability has been significant in influencing the rapid desiccation of the Aral Sea. From 1987 to 2014, relative humidity decreased from 64.76% to 61.15%, while air temperatures rose by more than 0.93°C (Massakbayeva et al., 2020). This warming trend significantly altered the regional climate, resulting in increased evaporation rates and decreased rainfall. The developments related to the Amu Darya and Syr Darya rivers exacerbated drought conditions by increasing water loss from the tributaries of the Aral Sea (Pan et al., 2022; Wang et al., 2024). Consequently, diminishing water supplies combined with rising evaporation rates led to a rapid decline in the water level of the Aral Sea.

Increased temperature extremes due to climate change have intensified the drying process. Precipitation decreases in winter, while summers experience increased heat stress, leading to accelerated soil moisture loss. Climatic instability affects soil salinization and degradation by diminishing natural leaching processes due to decreased rainfall, leading to salt accumulation on the exposed seabed. The analysis reveals that this effect

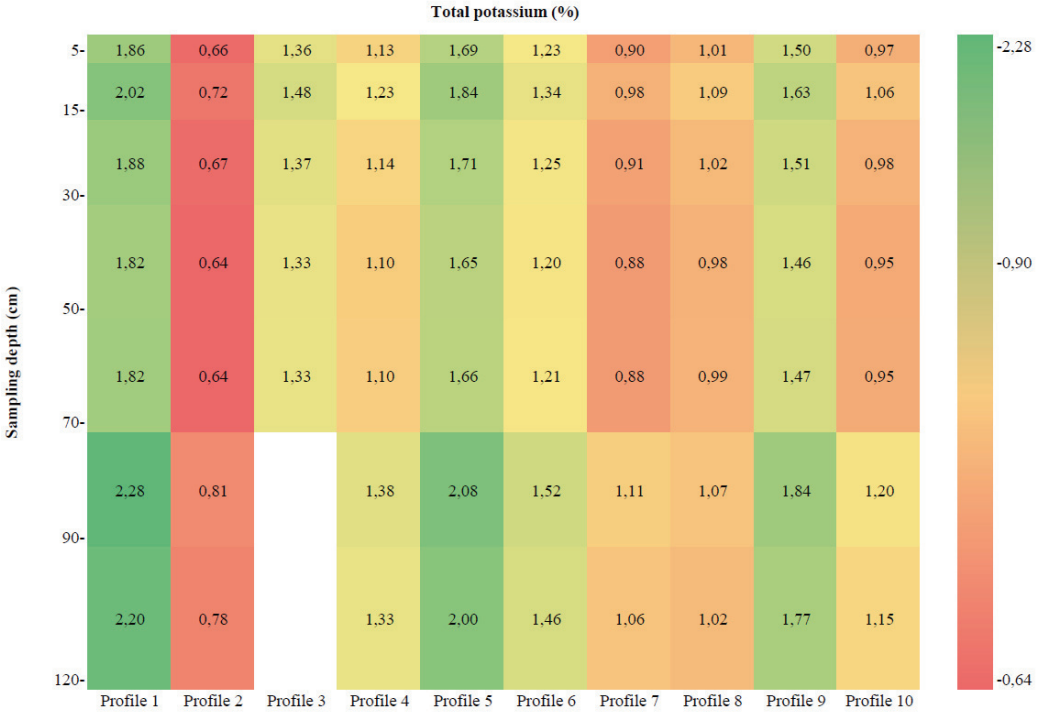

Fig. 8. Total potassium (%) distribution across profiles from the dried-up Aral Sea seabed

was especially significant in profiles exhibiting freshly exposed bottoms, where severe environmental conditions limited soil formation.

While climate change is significant, human activity primarily caused the drying up of the Aral Sea. Under Soviet-era agricultural policy, cotton farming led to substantial water diversions for large-scale irrigation projects, resulting in a significant reduction of outflows to the sea (Kayiranga et al., 2024). Approximately 82% of the diverted water is attributed to agriculture, indicating its significant role in this process (He et al., 2022). Minor fluctuations in water level were observed from 1920 to 1960; however, after 1960, the diversion of over 90% of the Aral Sea's inflow led to significant shrinkage (Micklin, 2014). By 1989, the Aral Sea had divided into the Big and Small Aral Seas, and by 2020, its surface area had decreased to nearly one-tenth of its original size (Yang et al., 2020). Ineffective irrigation technologies significantly increased water waste, as noted by Massakbayeva et al. (2020) , particularly through the use of unlined channels that are susceptible to high evaporation and seepage losses. The unsustainable activities have transformed the exposed seafloor into a barren landscape, currently generating dust. The presence of saline dust, augmented by toxic minerals and compounds, has significantly degraded soil quality and obstructed the development of stable soil profiles.

The Aral Sea issue is further complicated by social and geopolitical factors. The Soviet Union prioritized immediate economic gains from cotton exports at the expense of long-term environmental sustainability through the rapid construction of irrigation infrastructure. The competition for limited water resources has exacerbated regional tensions among downstream nations such as Uzbekistan and Kazakhstan, as well as upstream nations like Kyrgyzstan and Tajikistan (Micklin, 2016). The resultant environmental disaster has led to mass migration, public health issues, and significant economic stress in regions reliant on agriculture and fisheries. The desiccated seabed, laden with hazardous salts and chemicals, has generated dust storms that contribute to respiratory issues, cardiovascular diseases, and adverse effects on agricultural productivity, thereby exacerbating socioeconomic stress (Kumar, 2023; Lioubimtseva, 2023).

The phases of the Aral Sea's withdrawal were significant in shaping the development of soil across the exposed basin. The analysis of the soil profile in our investigation indicates varying tendencies that correspond to the timing of exposure and the evolving environmental conditions.

Profiles in the early drying parts of the Aral Sea, such as Profile 1, were characterized by finer textures, moderate salinity, and elevated organic matter content. While nutrient levels were high in this profile, similarly elevated values were also observed in intermediate (Profile 5) and recent (Profile 9) exposures, indicating no consistent age-related trend in nutrient distribution. The observed conditions suggest heightened vegetative input, ongoing leaching processes, and prolonged precipitation-driven infiltration, which facilitate more advanced soil formation (Ajiev et al., 2023; An et al., 2018; Issanova et al., 2022) .

Intermediate exposure profiles, specifically Profiles 2–5, exhibited a range of soil textures, distinct salinity patterns, and variable organic matter and nutrient content. The dynamic properties correspond to unstable hydrological conditions marked by alternating cycles of sediment deposition and waterlogging. Profile 5 exhibited elevated sand content in deeper layers, indicating that sediment redistribution was influenced by fluctuations in water levels (Kayiranga et al., 2024; Lioubimtseva, 2023).

Late exposure profiles, specifically Profiles 6 and 7, exhibited inconsistent salt levels, low to moderate organic matter content, and incomplete leaching patterns. The conditions indicate insufficient moisture retention and sporadic groundwater infiltration, thereby hindering stable soil formation (Gupta, 2020; Ismonov et al., 2024).

The most challenging conditions for soil growth were indicated by the latest exposure profiles (profiles 8–10). Rapid evaporation and inconsistent leaching processes resulted in profiles characterized by high salinity, low organic matter, and limited nutrient availability, particularly in Profiles 2, 3, and 7 (Kumar, 2023; Micklin, 2014; Zhu et al., 2024).

This study demonstrates a significant correlation between soil texture and exposure length, consistent with previous findings. Initial exposure profiles indicated increased clay accumulation and improved surface textures indicative of advanced pedogenesis (Ismonov et al., 2024; Issanova et al., 2023b; Kim et al., 2024). Conversely, profiles exhibiting later stages of exposure displayed coarser textures, indicating restricted pedogenic processes due to rapid moisture loss and surface salt accumulation.

Nutrient analysis did not confirm a consistent age-related trend. While earlier profiles, such as Profile 1, exhibited elevated nutrient levels, similarly high concentrations of nitrogen and phosphorus were also observed in intermediate (Profile 5) and recent (Profile 9) exposures. These findings suggest that nutrient accumulation is more closely linked to factors such as vegetation development, organic matter input, and localized microclimatic conditions, rather than the age of the sediments (Babur et al., 2022; Baturin et al., 2015; Gill et al., 2022).

It is also important to note that soil conditions did not uniformly improve or deteriorate within each exposure stage. For instance, among the intermediate profiles (2–5), Profile 5 demonstrated favorable nutrient and organic matter content, while Profiles 2 and 3 were markedly poorer. Similarly, Profile 9, despite being among the most recent exposures, exhibited nutrient and SOM levels comparable to much older profiles. This highlights the spatial heterogeneity of soil development within each stage and reinforces the need for restoration planning based on site-specific properties rather than general assumptions by exposure phase.

The lowered concentrations of soil organic matter and essential nutrients (nitrogen, phosphorus, potassium) in the 0–5 cm layer, compared to deeper layers, are primarily related to wind erosion and an accumulation of surface salts. The exposed seabed, lacking vegetation, is especially susceptible to aeolian processes that erode fine particles and organic matter from the topsoil. Additionally, the accumulation of wind-driven salts at the surface inhibits microbial activity and nutrient cycling. The identified constraints highlight the significance of surface management. The application of mulch may mitigate salinity

impacts, safeguard the soil from erosion and salt redeposition, and facilitate vegetation establishment by enhancing soil microenvironments.

Click or tap here to enter text.The findings highlight the need for restoration strategies that are specific to the site and adapted to the diverse soil conditions found on the exposed seafloor. Restoration planning should therefore be based on measured soil conditions—such as salinity, organic matter, and nutrient content—rather than drying stage alone, to ensure optimal plant selection and site performance. Early exposure profiles, such as Profile 1, with stable structures, moderate salinity (~7.8 dS·m^{-1}), finer textures, and relatively higher organic matter and nutrient levels, offer significant potential for the support of traditional salt-tolerant plants. The surface clay-silt composition enhances water retention, supporting more robust vegetative growth. In regions with limited water resources, the use of drought-tolerant species that necessitate minimal irrigation is advised. Appropriate species comprise resilient shrubs and trees, including tamarisk (*Tamarix spp.*), saxaul (*Haloxylon ammodendron*), and camelthorn (*Alhagi spp.*), all of which are adapted to arid environments.

Among the intermediate exposure profiles (Profiles 2–5), Profile 5 exhibited moderate salinity (~16.3 dS·m^{-1}), balanced loam texture, and higher nutrient and SOM levels, while Profiles 2 and 3 showed poor fertility, high salinity (~18–19.4 dS·m^{-1}), and coarser, sand-dominant subsoils. Therefore, restoration approaches in this group should be adjusted based on individual soil conditions. Where soil texture is supportive and fertility is moderate (e.g., Profile 5), moderately salt- and drought-tolerant grasses and shrubs such as saltbush (*Atriplex spp.*), feather grass (*Stipa spp.*), and sand ryegrass (*Leymus arenarius*), are recommended. In contrast, highly salt-tolerant pioneer species are more appropriate for severely degraded profiles such as 2 and 3.

Late exposure profiles (e.g., Profiles 6 and 7), characterized by moderate to high salinity and variable soil stability, show fluctuating salinity levels (e.g., Profile 6 ranges from 15.8 to 6.8 dS·m^{-1}), low to moderate organic matter, and mixed loamy textures. These conditions require halophytic plants capable of tolerating saline stress and anchoring less-developed soils. Species recommended for consideration include glasswort (*Salicornia spp.*), seepweed (*Suaeda spp.*), and seashore dropseed (*Sporobolus virginicus*), all of which exhibit resilience to periodic moisture stress.

Among the recent exposure profiles (Profiles 8–10), Profile 9 exhibited unexpectedly high nutrient and SOM levels, moderate clay-silt texture, and stable EC values (~15.7 dS·m^{-1}), while Profiles 8 and 10 were more degraded with erratic salinity and poor fertility. This variability suggests that even recently exposed areas may hold restoration potential if site-specific soil conditions are favorable. Profile 9 may support moderately salt-tolerant halophytes, while Profiles 8 and 10, with EC levels reaching up to 18.7 dS·m^{-1} and poor texture stability, require extreme halophytes that can establish in harsh conditions. Optimal restoration of these areas is achieved through the planting of highly salt-tolerant halophytes that can thrive in extreme conditions with limited soil development.Species recommended for saline desert environments include *Salicornia europaea*, *Salsola spp*., and *Halostachys belangeriana*, recognized for their resilience.

5. Conclusions

This study illustrates the substantial influence of drying stages on soil texture, salinity, organic matter, and nutrient distribution (N, P, K) at the dried up bottom of the Aral Sea, with critical implications for restoration planning. Soil sampling profiles from the earliest drying phases (e.g., Profile 1) exhibited finer textures, moderate salinity, elevated organic matter content, creating favorable conditions for the growth of drought- and salt-tolerant plants that require minimal irrigation. Intermediate drying phase profiles (Profiles 2–5) showed diverse soil textures and variable salinity and fertility, indicating the need for flexible strategies, from moderately salt-tolerant grasses to highly tolerant pioneers. Late exposure profiles, such as Profiles 6 and 7, exhibited elevated salinity levels, lower organic matter content, and fluctuating conditions, requiring targeted interventions with halophytic species capable of stabilizing unstable soils. Among the most recent drying phase profiles (Profiles 8–10), soil conditions were the most challenging—characterized by extreme salinity, low organic matter, and limited nutrient availability. However, exceptions such as Profile 9, which exhibited favorable fertility, highlight the importance of localized assessment.

The consistently reduced levels of soil organic matter and nutrients in the surface layer (0–5 cm), likely related to wind erosion and salt accumulation, indicate that surface mulching could mitigate salinity, enhance soil conditions, and promote more effective restoration positive results. The use of adaptive strategies, including the planting of drought-tolerant species in early exposure areas and the establishment of specialist halophytes in saline environments, improves restoration efforts through enhanced soil stabilization, reduced erosion, and increased biodiversity. These insights provide essential guidance for formulating sustainable restoration strategies to tackle persistent desertification issues in the Aral Sea region and comparable degraded ecosystems globally.

6. Limitations

This study has several limitations that should be acknowledged. The limited number of soil sample sites—only 10 profiles—restricted the development of a comprehensive vegetation-based restoration map, as these samples were predominantly located in the eastern and southeastern regions of the Aral Sea seabed. This restricted coverage fails to accurately represent soil variation across the entire exposed seabed. This study focused on evaluating soil characteristics for vegetation-based restoration; however, a deeper understanding of soil formation processes would require excavating profiles to greater depths. The initial objective was to assess seabed composition for restoration methods; however, the research team is cur-

rently focusing on soil formation techniques. Moreover, as no previous studies have classified these soils using the World Reference Base for Soil Resources (WRB), we applied national soil classification terminology in this study. Future research will aim to enhance vegetation mapping, broaden soil profile coverage, and apply WRB soil classification standards (IUSS Working Group WRB, 2022) to better support ecological restoration planning.

Acknowledgment

This study was supported by the Ministry of Higher Education, Science, and Innovation of the Republic of Uzbekistan under project number FL-8323102111, titled “Creating a scientific basis for grouping areas for planting plants according to the salinity, physical, chemical, and biological properties of the soils distributed in the dry bottom of the Aral Sea.”

Conflict of interest

The authors declare no conflict of interest. The authors declare that they have no known competing financial interests or personal relationships that could have appeared to influence the work reported in this paper. This research did not involve human or animal subjects.

Author Contributions

Zafarjon Jabbarov was responsible for conceptualization, funding acquisition, investigation, and writing—review & editing. **Shovkat Kholdorov** contributed to conceptualization, data curation, methodology, and writing—review & editing. **Urol Nomozov** was involved in soil sampling and laboratory analysis. **Samad Makhammadiev** participated in soil sampling and laboratory analysis. **Gulnora Djalilova** handled visualization, mapping, soil sampling, and laboratory analysis. **Shokhrukh Abdullaev** contributed to writing, soil sampling, and laboratory analysis.

All authors read and approved the final manuscript.

References

Ajiev, A.B., Mambetullayeva, S.M., Orazbayev, T.J., 2023. The current state of the soil cover formed on the dried-up bottom of the Aral Sea.

An, J., Kim, S., Chang, H., Khamzina, A., Son, Y., 2018. Vegetation establishment improves topsoil properties and enzyme activities in the dry Aral Sea Bed, Kazakhstan. Forestist 68, 1–6. https://doi.org/10.5152/forestist.2018.001

Babur, E., Dindaroğlu, T., Roy, R., Seleiman, M.F., Ozlu, E., Battaglia, M.L., Uslu, Ö.S., 2022. Chapter 9 – Relationship between organic matter and microbial biomass in different vegetation types, in: Pratap Singh, R., Manchanda, G., Bhattacharjee, K., Panosyan, H. (Eds.), Microbial Syntrophy-Mediated Eco-Enterprising. Academic Press, pp. 225–245. https://doi.org/https://doi.org/10.1016/B978-0-323-99900-7.00005-5

Baturin, G.N., Zavjalov, P.O., Friedrich, J., 2015. Geochemistry of sediments in the modern Aral Basin. Oceanology (Wash D C) 55. https://doi.org/10.1134/S0001437015020022

Brilliant Maps, 2023. The incredible shrinking Aral Sea 1960–2014 [WWW Document]. https://brilliantmaps.com/aral-sea/

Committee for Standardization and Metrology of the USSR, 1991. Soils. Methods for determination of organic matter. Moscow.

FAO, 2024. Global status of salt-affected soils – Main report. Rome.

Gill, A.L., et al., 2022. Nitrogen increases early-stage and slows late-stage decomposition across diverse grasslands. Journal of Ecology 110, 1376–1389. https://doi.org/10.1111/1365-2745.13878

Gupta, A., 2020. Shrinking of Aral Sea: An Environmental Disaster in Central Asia. International Journal of Humanities, Arts and Social Sciences 6, 162–170. https://doi.org/10.20469/ijhss.6.20003-4

He, H., Hamdi, R., Luo, G., Cai, P., Zhang, M., Shi, H., Li, C., Termonia, P., De Maeyer, P., Kurban, A., 2022. Numerical study on the climatic effect of the Aral Sea. Atmospheric Research 268, 105997. https://doi.org/10.1016/j.atmosres.2021.105977

Ismonov, A., Mamadjanova, U., Kattayeva, G., Rakhmonov, Z., 2024. The role of fluvial sediments in the formation of the Aral Sea dried bottom soils. Science and Innovation International Scientific Journal 3. https://doi.org/10.5281/zenodo.12107331

Issanova, G., Abuduwaili, J., Tynybayeva, K., 2023. Formation, Degradation, and Mapping, in: Issanova, G., Abuduwaili, J., Tynybayeva, K. (Eds.), Soil Cover of the Dried Aral Seabed in Kazakhstan. Springer Nature Switzerland, Cham, pp. 61–73. https://doi.org/10.1007/978-3-031-29867-7_5

Issanova, G., Abuduwaili, J., Tynybayeva, K., Kalybayeva, A., Kaldybayev, A., Tanirbergenov, S., Ge, Y., 2022. Assessment of the Soil Cover in the Dried Aral Seabed in Kazakhstan and Climate Change in the Region. Water Air and Soil Pollution 233. https://doi.org/10.1007/s11270-022-05966-2

IUSS Working Group WRB, 2022. World Reference Base for Soil Resources. International soil classification system for naming soils and creating legends for soil maps., 4th edition. ed. Vienna, Austria.

Kachinsky, N.A., 1943. Methods of mechanical and microagregatic analysis of soil. Publishing House Academy Science 39.

Kayiranga, A., Chen, X., Ingabire, D., Liu, T., Li, Y., Nzabarinda, V., Ochege, F.U., Hirwa, H., Duulatov, E., Nthangeni, W., 2024. Anthropogenic activities and the influence of desertification processes on the water cycle and water use in the Aral Sea basin. Journal of Hydrology: Regional Studies 51. https://doi.org/10.1016/j.ejrh.2023.101598

Kholdorov, S., Lakshmi, G., Jabbarov, Z., Yamaguchi, T., Yamashita, M., Samatov, N., Katsura, K., 2023. Analysis of Irrigated Salt-Affected Soils in the Central Fergana Valley, Uzbekistan, Using Landsat 8 and Sentinel-2 Satellite Images, Laboratory Studies, and Spectral Index-Based Approaches. Eurasian Soil Science 56, 1178–1189. https://doi.org/10.1134/S1064229323600185

Kim, Gaeun, Ahn, J., Chang, H., An, J., Khamzina, A., Kim, Gwangeun, Son, Y., 2024. Effect of vegetation introduction versus natural recovery on topsoil properties in the dried Aral Sea bed. Land Degradation & Development 35, 4121–4132. https://doi.org/https://doi.org/10.1002/ldr.5209

Kumar, Dr.S., 2023. Environment problems of the Aral Sea basin in central Asia and its impact on society, economy, and regional security. International Journal of Geography, Geology and Environment 5. https://doi.org/10.22271/27067483.2023.v5.i1b.191

Kuziyev, R., Abdurahmonov, N., Ramazonov, B., 2020. Soil resources of the Aral Sea region and the scientific basis for their effective use. Zilol-buloq, Tashkent.

Lioubimtseva, E., 2023. The Aral Sea disaster: revisiting the past to plan a better future, in: Biological and Environmental Hazards, Risks, and Disasters, Second Edition. https://doi.org/10.1016/B978-0-12-820509-9.00008-3

Massakbayeva, A., Abuduwaili, J., Bissenbayeva, S., Issina, B., Smanov, Z., 2020. Water balance of the Small Aral Sea. Environmental Earth Science 79, 75. https://doi.org/10.1007/s12665-019-8739-5

Micklin, P., 2016. The future Aral Sea: hope and despair. Environmental Earth Science 75, 844. https://doi.org/10.1007/s12665-016-5614-5

Micklin, P., 2014. Irrigation in the Aral Sea basin, in: The Aral Sea: The Devastation and Partial Rehabilitation of a Great Lake. https://doi.org/10.1007/978-3-642-02356-9_8

Ministry of Agriculture of the USSR, 1984a. Soils. Methods for determining total phosphorus and total potassium. Moscow.

Ministry of Agriculture of the USSR, 1984b. Soils. Methods for determination of total nitrogen. Moscow.

Pan, X., Wang, W., Liu, T., Akmalov, S., De Maeyer, P., Van de Voorde, T., 2022. Integrated modeling to assess the impact of climate change on the groundwater and surface water in the South Aral Sea area. J Hydrol (Amst) 614. https://doi.org/10.1016/j.jhydrol.2022.128641

UNESCO, 2017. Aral Sea and pre-Aral region summary of the work of the scientific research center of the UNESCO on monitoring the state and analyzing the situation. Baktria press, Tashkent.

United States Department of Agriculture, 1954. Diagnosis and improvement of saline and alkali soils. . Washington D.C.

Wang, X., Cui, B., Chen, Y., Feng, T., Li, Z., Fang, G., 2024. Dynamic changes in water resources and comprehensive assessment of water resource utilization efficiency in the Aral Sea basin, Central Asia. Journal of Environmental Management 353, 120198. https://doi.org/10.1016/j.jenvman.2024.120198

Yang, X., Wang, N., Chen, A., He, J., Hua, T., Qie, Y., 2020. Changes in area and water volume of the Aral Sea in the arid Central Asia over the period of 1960–2018 and their causes. Catena 191, 104566. https://doi.org/10.1016/j.catena.2020.104566

Zhu, H., Zheng, B., Zhong, W., Xu, J., Nie, W., Sun, Y., Guan, Z., 2024. Infiltration and Leaching Characteristics of Soils with Different Salinity under Fertilizer Irrigation. Agronomy 14. https://doi.org/10.3390/agronomy14030553